Original Bio-Based Antioxidant Poly(meth)acrylate from Gallic Acid-Based Monomers

Ali Khalil, Christine Gerardin-Charbonnier, Hubert Chapuis, Khalid Ferji, J.L. Six

Original Bio-based Antioxidant Poly(meth)acrylate from Gallic Acid -based Monomer

Ali KHALIL [a,b], *Christine GERARDIN-CHARBONNIER* [b,*], *Hubert CHAPUIS* [b], *Khalid FERJI* [a], *Jean-Luc SIX* [a,*]

a) Université de Lorraine, CNRS, LCPM, F-54000 Nancy, France

b) Université de Lorraine, INRAE, LERMAB, F-54000 Nancy, France

Submitted to ACS Sustainable Chemistry & Engineering

KEYWORDS: Photo-RAFT, Controlled polymerization, free radical scavenging, polyphenol, wood extractives.

ABSTRACT

Herein, we report a multistep synthesis of novel (meth)acrylate monomers based on gallic acid (GA), a bio-sourced phenolic acid. The objective of this work was to obtain bio-based polymers exhibiting antioxidant properties provided by monomers derived from gallic acid. The phenolic groups of GA, which are responsible for antioxidant properties, need to be protected for two reasons. On the one hand, functionalization to transform GA into polymerizable monomers must not take place at the phenolic groups because they must remain free to maintain the maximum antioxidant activity in the final polymers. On the other hand, their protection is necessary to prevent radical scavenging during the radical polymerization. After synthesis of such monomers, protected GA-based polymers were thus produced through a photo-mediated RAFT polymerization at room temperature by evaluating two trithiocarbonate-type chain transfer agents (CTAs). The kinetics and the molecular weight distributions were studied depending on the monomers and the CTAs. Protected polymers were then deprotected to afford polymeric chains carrying one free gallic acid moiety on each monomer unit. Antioxidant activity of these free GA-based polymers was demonstrated either through the DPPH free radical scavenging property and through the inhibition of the methyl linoleate oxidation.

INTRODUCTION

Secondary metabolites from plant kingdom or wood, have long been studied to harness their therapeutic properties. Indeed, according to recent studies, 25% of medicines are originated directly or indirectly from natural products.[1-3] These compounds correspond to polyphenols such as flavonoids, lignans, stilbenes, phenolic acids and nor tannins. Characterized by having at least one aromatic ring with one to several hydroxyl groups, polyphenols are widely diverse structurally and functionally.[4-6] Such phenolic bio-sourced compounds have been used in food applications, packaging or materials, or nor as multi-target bioactive agents against cancer and inflammation, but also in cosmetics and biofertilizers.[7-10] Gallic acid (GA, Scheme 1) is the most investigated polyphenol owing to its accessibility, applications and relatively low price. It can be extracted under different forms from chestnut, nuts, sumac, gallnuts, witch hazel, clove, tealeaves and other plants.[11] Moreover, it is particularly accessible *via* oak bark transformation industry under the form of hydrolysable tannins.[12-13] GA and its ester derivatives (e.g. propyl gallate, octyl gallate, and lauryl gallate) exhibit numerous properties serving as antioxidants, antimicrobials or anticancer, as well as active agents that reduce cellular oxidative stress.[14-16] However, concerning biomedical applications and similar to numerous phytochemicals, harnessing the full potential of GA within the human body stumbles with its low bioavailability and bioactivity which are pivotal for any bioactive molecule to be considered efficient.[17-19] To overcome these issues, drug delivery systems (DDSs) as polymeric electrospun fiber mats[20-22], nanoparticles[23-24] or hydrogels[25-28] have considerably grasped attention as a possible way to improve GA's pharmacokinetics.

Gallic acid, as an AB_3 tetra-functional monomer, has also inspired researchers to produce crosslinked[29-35] or hyperbranched polymeric materials.[36-38] Nevertheless, the conjugation of GA

onto natural polymeric substrates has received more significant attention. Moreover, a recent review has described the chemical/enzymatic grafting of GA onto polysaccharides to broaden applications in the fields of active packaging, edible coating and DDS.[39] Likewise, antioxidant properties of GA/gelatin conjugates were also reported.[40-41] Surprisingly, no GA-functionalized synthetic thermoplastic polymers were described despite the potential antioxidant properties of such materials. Nevertheless, strictly speaking, we must however point out i) the grafting of enzymatic-produced poly(gallic acid) onto polycaprolactone film to provide it antioxidant property[42]; and ii) gallol (1,2,3-trihydroxybenzene)-based polymers exhibiting antioxidant performances[43-46].

Since more than 30 years, many advanced and updated versions of reversible deactivation radical polymerizations (RDRP) including atom transfer radical polymerization (ATRP), nitroxide mediated polymerization (NMP), reversible addition-fragmentation chain transfer (RAFT) and few others have appeared.[47] RAFT polymerization, which is one of the most versatile and capable technique for polymer synthesis, has grasped significant attention from researchers yielding up more than 11,000 publications by the end of 2020.[48,49] Photo-mediated RAFT polymerization (photo-RAFT) has recently emerged as a versatile low-energy alternative of thermal one, due to its easiness, rapidity, ability to control the polymerization of a wide range of monomers at room temperature, and to afford spatio and temporal controls of the polymerization by switching the light on and off.[50-54] To the best of our knowledge, polymers issued from GA-based monomers have never been synthesized using photo-RAFT or any other RDRP mechanism. To date, only one paper reports the ring opening metathesis polymerization of GA-functionalized monomer.[55] The scarcity of papers dealing with such chain polymerizations may be undoubtedly linked to the difficulty of polymerizing GA-functionalized

monomers due to the presence of phenolic hydroxyl groups that are responsible of antioxidant property of GA. Protecting the hydroxyl group of GA before its radical polymerization can be an original way to obtain GA-based polymers *via* RDRP methods.

Within this framework, our focus is herein firstly devoted to the synthesis of two novel GA-based (meth)acrylate monomers. Homopolymers bearing one protected GA side group per monomer unit are then prepared from the corresponding monomers through photo-RAFT. After deprotection, GA moieties are afforded on the polymeric chains. Finally, the antioxidant activity of such novel polymers is studied using two different methods: 2,2-diphenyl-1-(2,4,6-trinitrophenyl)hydrazyl (DPPH) radical scavenging assay and inhibition of methyl linoleate oxidation.

EXPERIMENTAL SECTION

Materials

Methyl gallate (1, Scheme 1) (99%, Acros Organics) and N-(3-dimethylaminopropyl)-N′-ethylcarbodiimide hydrochloride (EDC.HCl, 99%, ABCR) were used as received. Benzyl bromide (98%), 4-(dimethylamino)pyridine (DMAP, 99%), 2-hydroxyethyl acrylate (96%), 2-hydroxyethyl methacrylate (99%), N-hydroxyethyl acrylamide (97%,), palladium on carbon (Pd/C, 10 wt. % loading), methyl linoleate (98%), 2,2-diphenyl-1-(2,4,6-trinitrophenyl)hydrazyl (DPPH, 95%), potassium carbonate (K_2CO_3), potassium hydroxide (KOH), sodium bicarbonate ($NaHCO_3$), magnesium sulfate ($MgSO_4$), filter agent Celite® 545 were ordered from Merck and used as received. Dimethyl sulfoxide (DMSO, 99.7%, Merck) was stored with molecular sieves.

Acetone (99.8%), dichloromethane (99.9%), hexane (96%) and methanol (99.9%) were purchased from Carlo Erba, when acetonitrile (99.8%), 1-butanol (99.8%), ethyl acetate (99%) were from Merck. All these solvents were used as received. Azobisisobutyronitrile (AIBN, 98%, Merck) was recrystallized from methanol and dried overnight at 40 °C under vacuum. Chain transfer agents (CTAs, Figure 1) were prepared as previously reported.[50, 56] Ethyl (2,4,6-trimethylbenzoyl) phenylphosphinate (TPO-L, Figure 1) was purchased from Fluorochem and used as received.

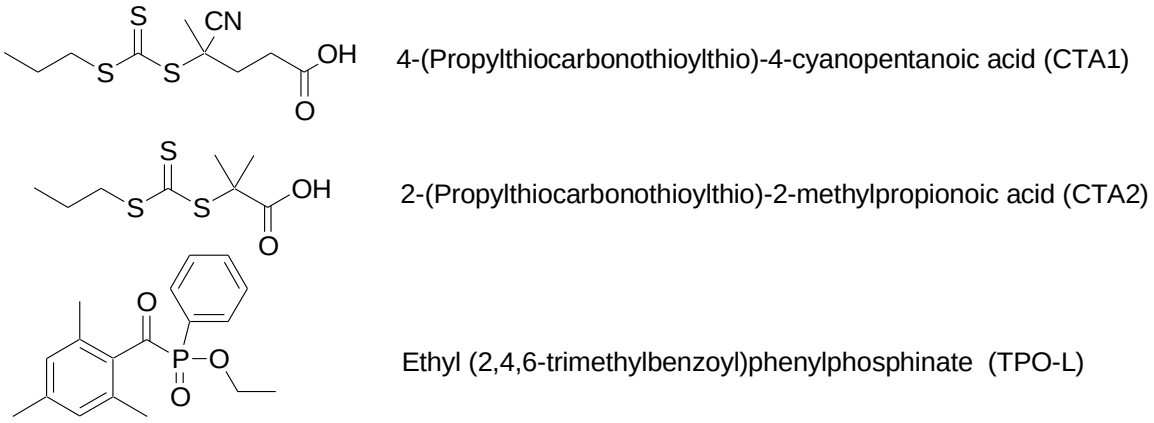

Figure 1. CTAs and photoinitiator used in the present study.

Perbenzylated acrylate (BnGA-A) and methacrylate (BnGA-MA) monomers (Scheme 1)

3,4,5-tribenzyloxybenzoic acid (3) was synthesised from methyl gallate (1) according to an improved procedure from previous reports.[57-58] Accordingly, (1) was benzylated in the presence of 3.5 equivalents of benzyl bromide in mild basic conditions (K_2CO_3) at 60°C. Then, the benzylated compound (2) was hydrolysed in strong basic conditions (KOH) at reflux to obtain (3) with a good yield. ^{1}H NMR spectra of compounds (1), (2) and (3) are given in Figure S1.

In a round bottom flask, 1 eq. of (3), 1.1 eq. of EDC.HCl and 0.15 eq. of DMAP were dissolved in 200 mL ethyl acetate. After cooling at 4°C, 1 eq. of 2-hydroxyethyl acrylate or 2-hydroxyethyl methacrylate was slowly added. The mixture was stirred for 30 minutes, then left at room temperature. The reaction progress was monitored by thin layer chromatography (see below for used eluants), then the reaction medium was washed twice with 100 mL distilled water followed by saturated $NaHCO_3$ aqueous phase. The organic phase was dried under $MgSO_4$ then concentrated under vacuum. Pure monomers (perbenzylated acrylate (BnGA-A) and perbenzylated methacrylate (BnGA-MA)) were recovered as white powders by silica gel column purification using different eluants depending on the nature of the monomer: dichloromethane/acetone (7/3 v/v) was used for BnGA-A (R_f=0.78, 60% yield) and ethyl acetate/hexane (5/5 v/v) for BnGA-MA (R_f=0.82, 55% yield). ^{1}H NMR spectra of perbenzylated GA-based monomers are shown on Figure 2. ^{13}C NMR and FTIR spectra are given in supporting information (Figures S2 and S3, respectively).

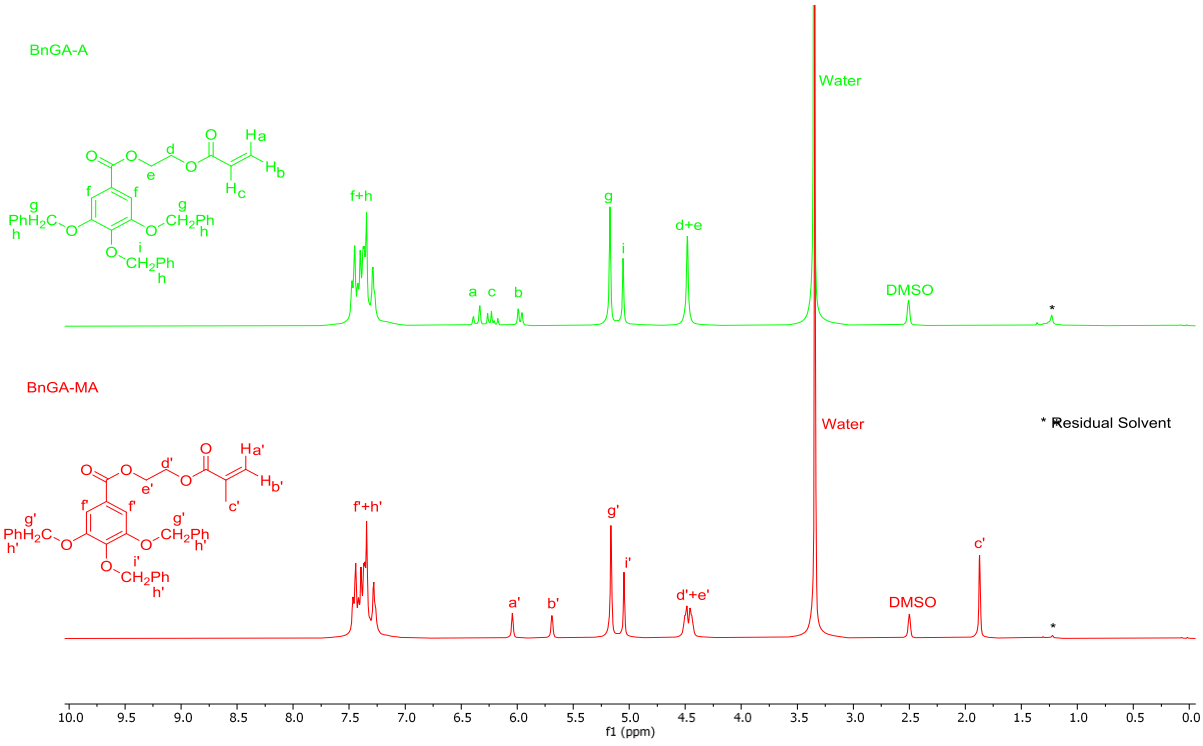

Figure 2. ^{1}H NMR spectra (DMSO-d_6) of BnGA-A and BnGA-MA.

Polymerizations

In a typical polymerization procedure, 500 mg (200 eq.) of the monomer (BnGA-A or BnGA-MA) were solubilized in DMSO (1 mol/mL) in a 15 mL vial followed by the addition of 1 eq. of AIBN in case of conventional radical polymerization. The reaction medium was purged with a continuous flow of nitrogen for 15 min. The vial was then immersed in a thermostated oil bath at 70°C to initiate the polymerization. In case of photo-RAFT, 1 eq. of CTA (CTA1 or CTA2, 100 mg/mL in DMSO) was added in the vial instead of AIBN, then 0.33 eq. of the photoinitiator TPO-L (20 mg/mL in DMSO) per CTA. After purge, the medium was finally irradiated with homemade UV-VIS LED lamp (405 nm, 10 $mWcm^{-2}$) at room temperature during maximum 2 hours to initiate and propagate the polymerization.

In each case, 200 µL of the reaction medium were withdrawn under nitrogen at different time and analyzed by ^{1}H NMR and SEC. Monomer conversion (x) was determined by ^{1}H NMR according to equations given in Table S1, by comparing the peaks areas of the ethylenic protons of the monomer (from 5.60 to 6.45 ppm) with those of the aromatic protons (centered at 7.20 ppm) of both monomer and polymer. Example of BnGA-MA is given in Figure S4. After polymerization, crude polymers P(BnGA-A) and P(BnGA-MA) were precipitated from acetonitrile, then dried under vacuum at 50^{0} C.

Hydrogenolysis of perbenzylated polymers

1 g of protected polymer was dissolved in 30 mL of methanol/ethyl acetate (60/40, v/v) at room temperature in a stainless-steel autoclave (series 4560 mini-reactor from Parr Instrument Compagny) prior to the addition of 10 %wt. Pd/C. The reactor was sealed, firstly flushed with N_2

then several times with H_2, and finally placed under H_2 pressure (25 bars). The reaction mixture was then allowed to stir at room temperature for 48 hours before the reactor was vented to atmospheric pressure. The crude mixture was then filtered through Celite by using ethanol. Dialysis in methanol was performed to purify the free GA-based polymer that is concentrated under reduced pressure to obtain greyish white solid. Dialysis membranes were purchased from Spectra Por (MWCO: 6000–8000).

DPPH scavenging activity assay

Free gallic acid-based polymer stock solutions (25 mM of GA-based monomer units in methanol) were serially diluted to different concentrations (5, 2.5, 1, 0.5, 0.1, and 0.05 mM). A DPPH solution (91 μM in methanol) was freshly prepared. The polymer solutions (30 μL) were added to 3 mL of DPPH solution and allowed to react at room temperature. The final concentrations of GA unit were 0.5, 1, 5, 25, 10, 50 μM. Same concentrations of gallic acid were also used. After 12 min, the absorption value (A_{sample}, measured at 517 nm by UV-visible spectrometry) ceased to decrease. A_{final} is the absorption value of the DPPH solution using an excess amount of the antioxidant moieties, measured after the same reaction time. DPPH/methanol (91 μM, 3mL) was considered as control to determine the value of A_{blank}. The DPPH scavenging capacity (% of reduction of DPPH radical) was calculated according to Eq. 1:

$$\text{DPPH Radical Reduction (\%)} = \frac{A_{blank} - A_{sample}}{A_{blank} - A_{final}} \times 100 \quad (1)$$

C_{50} value was estimated as the concentration of antioxidant for 50% DPPH scavenging by plotting DPPH radical reduction *vs* concentration. All experiments were performed in triplicates.

Oxygen uptake method

In a typical procedure, 1 mL of the antioxidant solution in DMSO (0.8 mM of GA or GA-based monomer unit) was introduced into a thermostatically controlled reactor. No antioxidant

was introduced for the control assay but rather 1 mL of DMSO instead. 1 mL of methyl linoleate (1.6 M in 1-butanol) and 2 mL of AIBN (18 mM in 1-butanol) solutions were added, then the temperature was set to 60°C. The reaction was continued for 2.5 hours under an initial oxygen pressure ($P_0(O_2)$) of about 145 Torrs (0.193 bars). Oxygen uptake was monitored continuously by a pressure transducer. After 2.5 hours, the amount of oxygen consumed under these conditions ($\Delta P = P_0(O_2) - P_{2.5\ hours}(O_2)$) was compared to that consumed during the control reaction. The oxygen uptake inhibition index (OUI) is a characteristic to the antioxidative capacity of the sample and is estimated according to Eq. 2. Strong and poor antioxidants exhibit OUI values equal to 100% and 0%, respectively.

$$\text{OUI}\ (\%) = \frac{\Delta P_{\text{control}} - \Delta P_{\text{sample}}}{\Delta P_{\text{control}}} \times 100 \qquad (2)$$

Instruments and measurements

^{1}H, JMOD ^{13}C NMR spectra were recorded on a Bruker Advance 300 spectrometer (300.13 MHz, 298°K) in DMSO-d_6.

Fourier-transform infrared spectroscopy (FTIR) analyses were performed on Frontier FT-IR Spectrometer Perkin Elmer with Diamond ATR module.

Molar mass distributions of perbenzylated polymers were estimated by size exclusion chromatography (SEC) in THF at 40 °C (elution rate 1 mL/min) equipped with a multi-angle laser light scattering detector (MALLS; Mini Dawn Treos, Wyatt), a differential refractometer detector (OPTILab Rex, Wyatt), a HPLC pump (Waters 515), a degasser AF (Waters In-Line), and three PLgel 5 µl (10^5, 10^3, and 100 Å) columns (300×7.5 mm^2). dn/dc values of 0.185 and 0.230 were estimated for P(BnGA-A) and P(BnGA-MA), respectively. In case of deprotected polymers, SEC was carried out in DMSO containing $NaNO_3$ (8.5 g/L) as eluent at 70 °C (elution rate 0.7 mL/min), equipped with a differential refractometer detector (RID 10A, Shimadzu), a

HPLC pump (LC 20AD, Shimadzu), a degasser AF (DGU – 20A3R, Shimadzu), and three PLgel 5 µL columns (see above). SEC instrument (DMSO/$NaNO_3$) was calibrated with narrow linear poly(methyl methacrylate) (PMMA) standards.

UV-visible spectrometry analyses were performed using Lambda 365 UV-Vis Spectrophotometer – Perkin Elmer and quartz cuvettes.

Differential scanning calorimetry analyses (DSC) were carried out on DSC Q2000 from TA Instruments. Three cycles were successively recorded under nitrogen: the heating rate was 10°C/min while the cooling rate was 5°C/min. The temperature was varied from −40°C up to 180°C. First cycle was used to remove all thermal history from the sample. The second heating cycle was used for determining the glass transition temperature at the inflexion point. Analysis of the data was performed using Universal® Analysis 2000 (version 4.5A) software.

Thermogravimetric Analysis (TGA) analyses were performed on a Metler Toledo TGA/DSC1-TMA/SDTA 84Xe instrument by heating the polymer samples at a rate of 10^0 C/min from 25 to 600^0 C under a dynamic nitrogen atmosphere (flow rate =10mL/min).

RESULTS AND DISCUSSION

Perbenzylated gallic acid-based monomers

As previously explained, GA is an efficient natural antioxidant able to rapidly inhibit radicals due to the high stability of the radical forms of GA.[59] We hypothesized that radical polymerization of a GA-based monomer can be very difficult. In order to check this hypothesis, methyl methacrylate (MMA) was polymerized as model monomer in the presence of GA (1 eq.) through a thermally initiated free radical polymerization at 70°C using AIBN as initiator (data not shown). As predicted, polymerization of MMA was very slow due to the retardation effect of

phenolic hydroxyl groups of GA. Therefore, protection of the 3 hydroxyl functions of GA is required to reach high monomer conversion of the GA-based monomers. For this aim, on the one hand, benzyl protector group was selected given its very common use for this protection. On the other hand, two polymerizable model functions (acrylate and methacrylate) were linked to the protected GA.

Perbenzylated acrylate (BnGA-A) and perbenzylated methacrylate (BnGA-MA) monomers were prepared in two steps (Scheme 1). Firstly, 3,4,5-tribenzyloxybenzoic acid (3) was prepared then esterified with 2-hydroxyethyl(meth)acrylate in the presence of EDC.HCl and DMAP to prepare new protected GA-based acrylate and (meth)acrylates (BnGA-A and BnGA-MA). ^{1}H NMR spectra of BnGA-A and BnGA-MA (Figure 2) displayed multiplets between 4.30 and 4.60 ppm that correspond to the four protons between the two ester functions. Ethylenic protons are observed between 5.60 to 6.45 ppm, when the chemical shift of the methyl protons of BnGA-MA is 1.87 ppm. Aromatic protons are observed from 7.00 to 7.60 ppm, when benzylic protons displayed two peaks at 5.05 and 5.16 ppm. Integration of all these various peaks confirmed the good functionalization of BnGA-A and BnGA-MA.

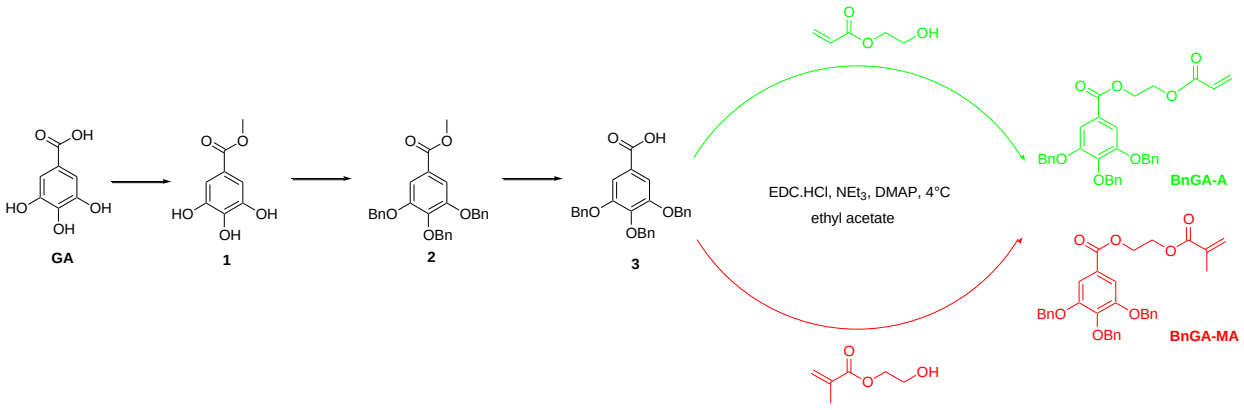

Scheme 1. Synthesis of perbenzylated GA-based monomers.

Polymerization of perbenzylated GA-based monomers

On the first hand, the free radical homopolymerization of BnGA-A and BnGA-MA was carried out in DMSO at 70°C using AIBN to check the polymerizability of these novel perbenzylated monomers. Aliquots of the reaction mixture were withdrawn to follow the polymerization kinetics by ^{1}H NMR. As shown in Figure S4, the ^{1}H NMR spectrum of the crude medium of the polymerization of BnGA-MA within 2 hours confirms the decrease of the ethylenic protons peaks with respect to that of aromatic ones during the polymerization. The plot of the monomer conversion (x) *vs* time (Figure 3A) shows different rates of polymerization. High conversion (96%) was achieved within 22 hours for BnGA-MA when lower conversion was observed for BnGA-A indicating the presence of radical deactivation reactions. However, whichever the monomer was, the evolution of the first-order kinetic plots *vs* time (Figure 3B) was not linear in agreement with an uncontrolled free radical polymerization. After 22 hours of polymerization, SEC traces of polymers derived from BnGA-A and BnGA-MA (P(BnGA-A) and P(BnGA-MA), respectively) are given in Figure S5 and the molecular weight distributions are resumed in Table 1.

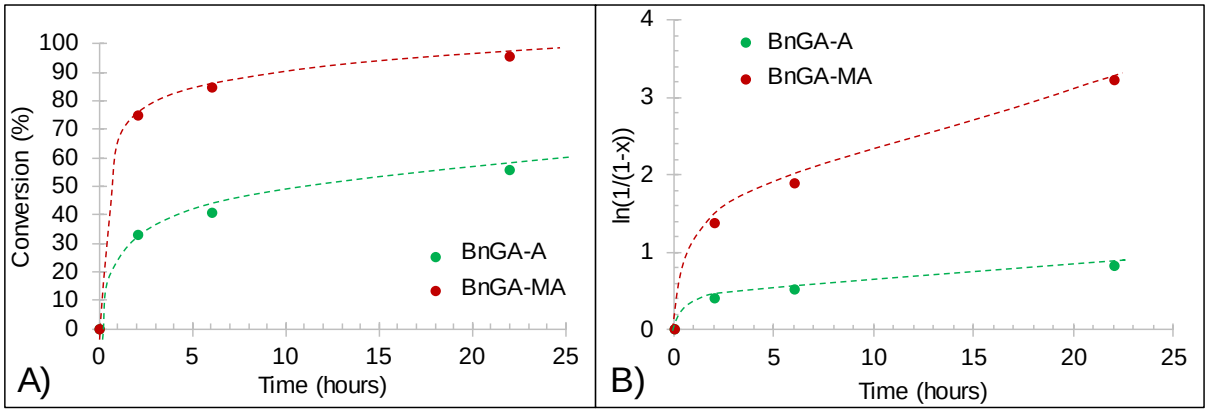

Figure 3. Monomer conversion (A) and semilogarithmic (B) plots *vs* time during the polymerization of BnGA-A and BnGA-MA initiated by AIBN in DMSO at 70°C.

Table 1. Free radical polymerization and photo-RAFT polymerizations in DMSO (1 mol/mL) of BnGA-A and BnGA-MA.

Monomer	System	Conversion (%) [c]	$\overline{M_{n_{NMR}}}$(kg/mol) [d]	$\overline{M_{n_{SEC}}}$ (kg/mol) [e]	Đ [e]
BnGA-A	AIBN [a]	56	60.28	34.70	1.31
	CTA1 [b]	46	49.79	49.00	1.15
	CTA2 [b]	55	59.44	38.90	1.13
BnGA-MA	AIBN [a]	96	106.10	210.00	1.57
	CTA1 [b]	89	98.64	93.00	1.26
	CTA2 [b]	90	99.70	68.46	1.24

a) $[M]_0/[AIBN]_0$=200/1 at 70^0 C during 22 hours.

b) $[M]_0/[CTA]_0/[TPO\text{-}L]$ = 200/1/0.33 at 405 nm irradiation during 2h at RT.

c) Conversion determined by ^{1}H NMR according to equations given in Table S1.

d) $\overline{M_{n_{NMR}}} = \text{conversion} \times M_0 \times 200 + M_{CTA}$, with M_0 the respective molecular weight of monomer unit (M_0^{BnGA-A}: 538.22 g/mol, $M_0^{BnGA-MA}$: 552.60 g/mol) and M_{CTA} the respective molecular weight of CTA (M_0^{CTA1}: 277.43 g/mol, M_0^{CTA2}: 238.03 g/mol).

e) Experimental number average molar mass and dispersity estimated by SEC analysis in THF at 40^0 C.

On the other hand, photo-RAFT of both monomers was investigated in DMSO at RT (Scheme 2) as this technique was proven to be an effective route for the polymerization of (meth)acrylic monomers as we already reported.[50-52, 56, 60-61] Accordingly, in the present study, the photo-RAFT of BnGA-A and BnGA-MA were carried out using initial molar ratios $[CTA]_0/[TPO\text{-}L]_0$ = 3 and

$[M]_0/[CTA]_0 = 200$, and the visible light (405 nm) was used to activate decomposition of TPO-L (Figure S6) and to prevent CTAs from photolysis reaction.[52, 61]

Table 1 summarizes the conversion, the molar masses and dispersity obtained for each case. ^{1}H NMR spectra of P(BnGA-A) and P(BnGA-MA) are shown in Figures 4 and S7. In case of BnGA-MA monomer, the ^{1}H NMR spectrum of pure P(BnGA-MA) shows the complete disappearance of vinylic hydrogens at 5.69 at 6.05 ppm (Figure 4). Moreover, the chemical shifts of benzylic protons (i, g and h), as well as those of protons d and e, have shifted to lower ppm upon polymerization with the appearance of new aliphatic main-chain protons below 2 ppm. ^{13}C NMR spectra of these compounds are drawn in Figure S8 and support again the disappearance of the C=C bond of the monomers (shift of the ethylenic C peaks from 125-135 ppm range (Figure S2) to alkyl ones around 20 ppm). FTIR spectra confirm also the disappearance of vinylic C=C band around 1635 cm^{-1} (Figure S3).

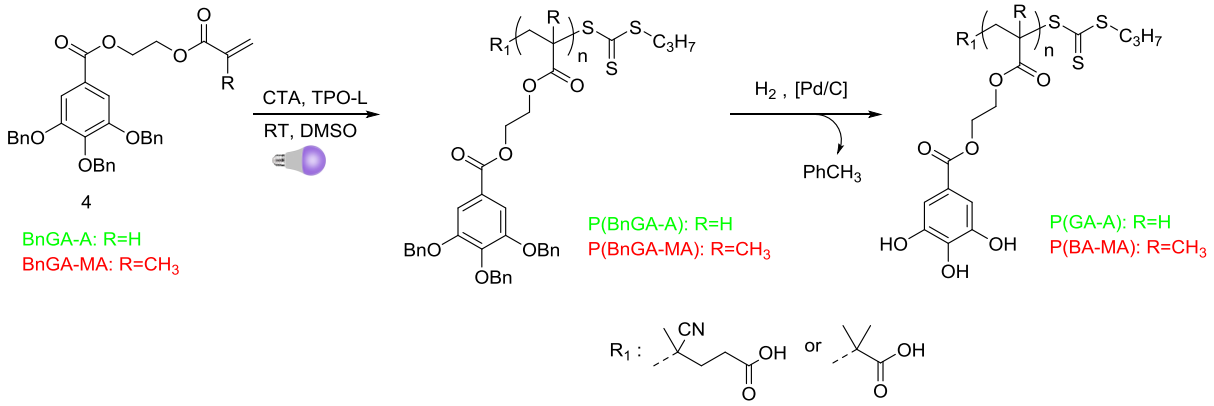

Scheme 2. Synthesis of free GA-based polymers through photo-RAFT of BnGA-A and BnGA-MA.

We firstly investigated the influence of the chain transfer agent in the presence of TPO-L as photoinitiator. The first-order kinetic plots *vs* time of polymerization performed with CTA1 or

CTA2 are shown in Figures 5A and 5B. Whichever the CTA used, uncontrolled polymerizations of BnGA-A occur reaching moderate conversion rates (46-55%) after 2 hours of irradiation. Such conversions are very similar to those observed using AIBN to initiate the free radical polymerization (Figure 3B). Surprisingly, the polymerizations of BnGA-A were not as efficient as expected although CTA2 is known to be more compatible with acrylates than methacrylates. However, by comparing the SEC traces of P(BnGA-A) obtained from polymerization using these two CTAs after 2 hours, one can observe a pic referring to dead chains of high molar masses in the case of CTA1 (Figure S9) and not with CTA2. Note that the amount of such dead chains (with CTA1) is very limited in comparison to the free thermal polymerization in the presence of AIBN (Figure S5). Such dead chains can be explained by a lower reactivity of this acrylate-based monomer inducing some limited free radical polymerization at early stage of polymerization before the establishment of the main RAFT equilibrium.

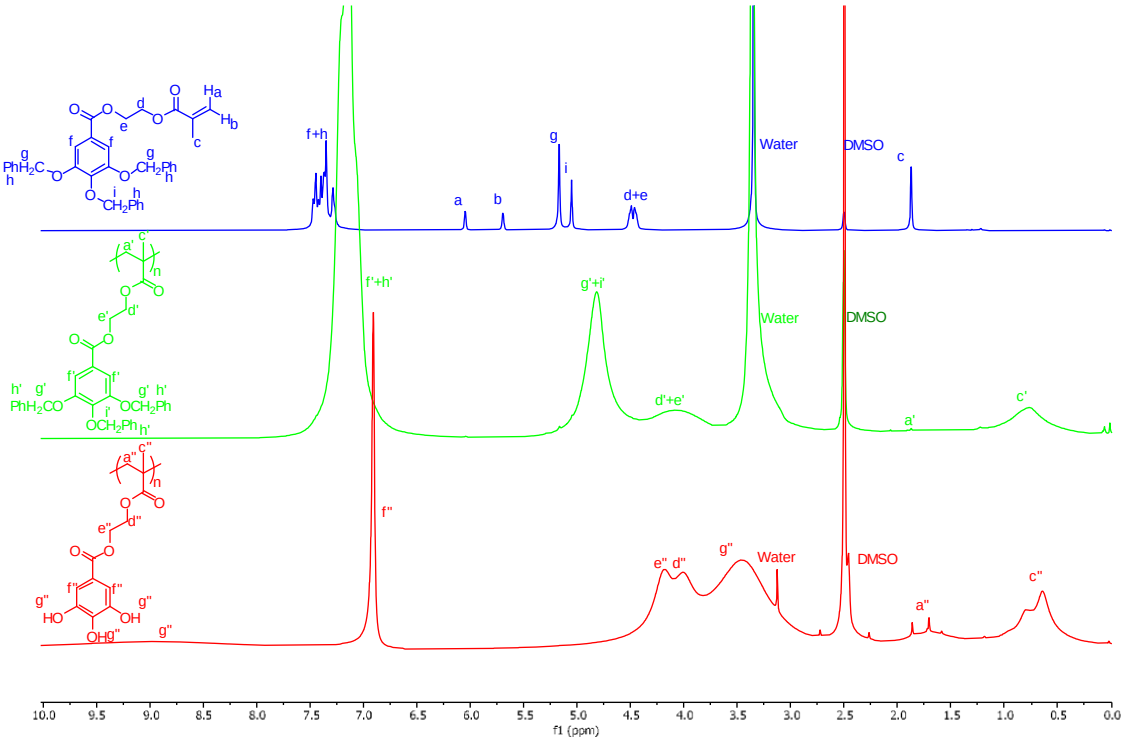

Figure 4. ^{1}H NMR spectra (DMSO-d_6) of BnGA-MA (Blue), P(BnGA-MA) (Green) and P(GA-MA) (Red).

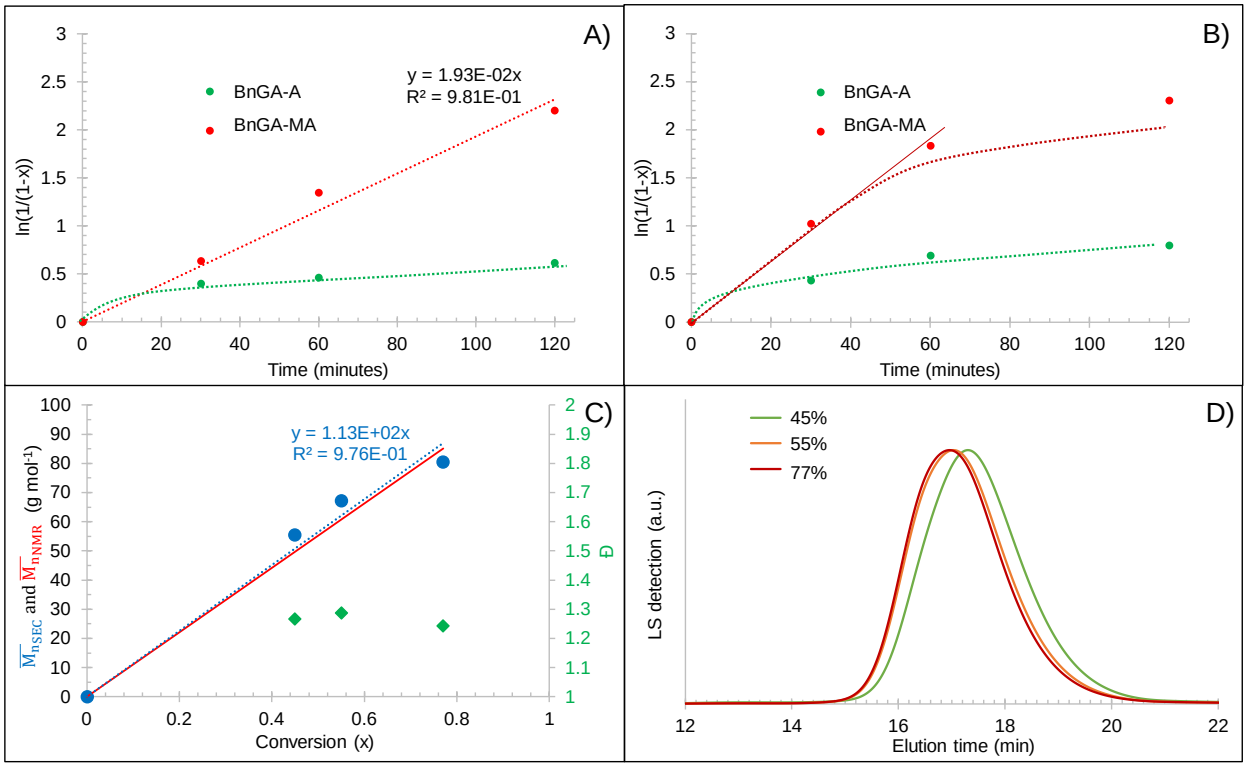

Figure 5. Semilogarithmic plots *vs* polymerization time during the photo-RAFT using CTA1 (A) or CTA2 (B) as chain transfer agent. $[M]_0/[CTA]_0/[TPO\text{-}L]_0$=200/1/0.33, DMSO, RT, 405 nm. (C) Plots of $\overline{M_{n_{SEC}}}$, $\overline{M_{n_{NMR}}}$ and Đ *vs* conversion and (D) SEC traces evolution (LS detection) in the case of photo-RAFT polymerization of BnGA-MA carried out with CTA1.

As shown in Table 1, almost 90% of BnGA-MA conversion was reached after 2 hours of polymerization whichever the CTA used. A linear first-order kinetic is observed until 89% of monomer conversion (2 hours of polymerization, Figure 5A) with CTA1, whereas the linearity was lost after 1 hour in the presence of CTA2 (84% of conversion, Figure 5B). SEC analysis

after 2 hours of polymerization confirm this lost control with CTA2 as $\overline{M_{n_{SEC}}}$ and $\overline{M_{n_{NMR}}}$ are not in agreement in such a case (Table 1). However, our results are suggesting that both CTA are efficient to control the photo-RAFT of BnGA-MA. Example of the evolution of the molecular weight and dispersity *vs* monomer conversion are shown in Figures 5C and 5D (PBnGA-MA prepared in the presence of CTA1). Consistent experimental molecular weights estimated by both ^{1}H NMR and SEC ($\overline{M_{n_{NMR}}}$ and $\overline{M_{n_{SEC}}}$) were recorded throughout the conversion range. The low dispersities (Đ =1.3) and the shift of chromatograms toward low elution time recorded at different conversion demonstrate the control of the photo-RAFT of BnGA-MA when using CTA1/TPO-L system. Finally, we investigated the chain-end fidelity within this system. BnGA-MA was polymerized using CTA1 and TPO-L up to 50% conversion. The polymer was then purified ($\overline{M_{n_{SEC}}}$=52700 gmol^{-1}, Đ=1.18) and used as a macro-CTA to initiate a new polymerization of BnGA-MA. The polymerization proceeded with 20% conversion. SEC analysis of the final polymer ($\overline{M_{n_{SEC}}}$=83600 gmol^{-1}, Đ=1.27, Figure 6) showed a shifted trace toward lower elution time without a significant increase of the dispersity, supporting the high efficiency of such controlled photo-RAFT of BnGA-MA.

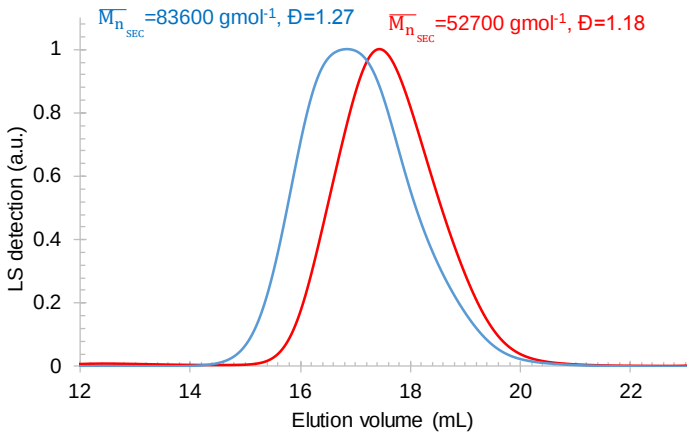

Figure 6. Evolution of SEC traces (LS detection) after a sequential polymerization of BnGA-MA. $[M]_0/[CTA1]_0/[TPO\text{-}L]_0$=200/1/0.33, DMSO, RT, 405 nm.

Free GA-based polymers

In the following step, free GA-based polymers (P(GA-A) and P(GA-MA)) were obtained after the deprotection of previous perbenzylated P(BnGA-A) and P(BnGA-MA) that were produced after 2 hours by photo-RAFT. Heterogenous Pd/C catalysis was used under relatively mild conditions (H_2 pressure =25 bars, RT, 48h) to deprotect each repeating unit of the protected polymers (Scheme 2). The free GA-based polymers were recovered by dialysis purification in methanol (limited options of dialysis solvent due to the polymer solubility) as light-greyish white to light-yellowish white solids (60% yields). To support the appearance of the free GA moiety per monomer unit on the different polymers, ^{1}H and ^{13}C NMR spectra were registered. Figures 4 and S7 demonstrate the total disappearance of the benzyl protecting groups (peaks g', h' and i') and the shift of the aromatic peak (f") to 6.8 ppm which is consistent with the aromatic protons of free GA (Figure S1). The total disappearance of the protecting groups was also evidenced by the ^{13}C NMR spectra (from 125 to 140 ppm) after the hydrogenolysis (Figures S8 *vs* S10) when the aromatic C (peaks 9 and 10) shifted to lower ppm, in accordance with the ^{13}C NMR of gallic acid. As shown in Figure S3, FTIR analyses of P(GA-A) and P(GA-MA) showed the appearance of bands around 3250 cm^{-1} corresponding to O-H stretch absorption. SEC traces of free GA-based polymers are reported in Figure 7. SEC analysis was done in DMSO/$NaNO_3$ due to the lack of solubility of free GA-based polymers in THF. After hydrogenolysis of benzyl protecting groups, an increase of the dispersity values has been registered (Table 2) in agreement with both the establishment of many hydrogen bonds between the numerous phenolic functions of the

polymeric chains and the possible adhesion of the chains onto the column. The difference between $\overline{M_{n_{NMR}}}$ and experimental $\overline{M_{n_{SEC}}}$ values was related to the use of PMMA calibration.

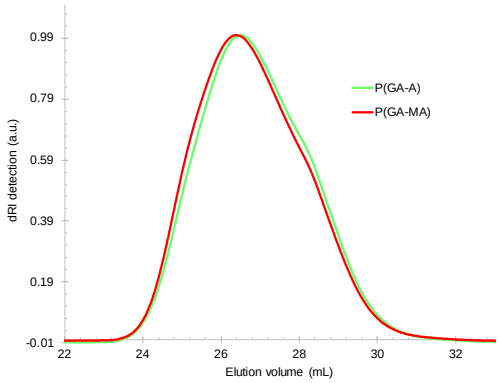

Figure 7. SEC traces (LS detection) of P(GA-A) and P(GA-MA).

Table 2. Molecular and thermal characterization of polymers before and after deprotection.

Perbenzylated polymers				
Polymer[a]	$\overline{M_{n_{NMR}}}$ (kg/mol)[b]	$\overline{M_{n_{SEC}}}$ (kg/mol)[c]	$Đ$ [c]	T_g (^{0} C) [d]
P(BnGA-A)	59.44	38.90	1.24	35.8
P(BnGA-MA)	98.64	93.00	1.26	28.1
Free GA-based polymers				
Polymer	$\overline{M_{n_{NMR}}}$ (kg/mol)[e]	$\overline{M_{n_{SEC}}}$ (kg/mol)[f]	$Đ$ [f]	T_g (^{0} C) [d]
P(GA-A)	29.74	184.70	1.56	129.5
P(GA-MA)	50.58	296.20	1.51	127.2

a) P(BnGA-A) (P(BnGA-MA)) were obtained by photo-RAFT after 2 hours of irradiation (see Table 1).

b) $\overline{M_{n_{NMR}}} = \text{conversion} \times M_0 \times 200 + M_{CTA}$, with M_0 the respective molecular weight of monomer unit (M_0^{BnGA-A}: 538.22 g/mol, $M_0^{BnGA-MA}$: 552.60 g/mol) and M_{CTA} the respective molecular weight of CTA (M_0^{CTA1}: 277.43 g/mol, M_0^{CTA2}: 238 g/mol).

c) Experimental number average molar mass and dispersity estimated by SEC analysis in THF at 40°C.

d) Glass transition temperature measured using the 2nd heating cycle.

e) $\overline{M_{n_{NMR}}} = \text{conversion} \times M'_0 \times 200 + M_{CTA}$, with M'$_0$ the respective molecular weight of deprotected monomer unit (M_0^{GA-A}: 268.22 g/mol, M_0^{GA-MA}: 282.60 g/mol)

f) Experimental number average molar mass and dispersity estimated by SEC analysis in DMSO/$NaNO_3$ at 70^0 C. (SEC traces in Figure 7).

Thermal characteristics of perbenzylated-GA and free GA based polymers

The thermal characteristics of the perbenzylated polymers and their corresponding free GA-based polymers were determined by DSC and TGA (Table 2). As expected, P(BnGA-A) shows a higher Tg value than the polymethacrylate P(BnGa-MA) (35.8°C *vs* 28.1°C). After deprotection, Tg increased by almost 100°C to reach 129.5°C in case of P(GA-A) and 127.2°C in case of P(GA-MA), due to the establishment of many hydrogen bonds between the numerous phenolic functions of the polymeric chains and the significant decrease in the steric hindrance around the polymer backbone. Thermo-gravimetric analysis (TGA) revealed a similar behaviour for the two perbenzylated polymers with an initial loss of mass upon heating at about 250^0 C (Table 2, Figure S11). Such protected polymers showed higher thermal stability than the deprotected ones bearing free GA moieties as P(GA-A) and P(GA-MA) gradually degraded when the temperature was over Tg for P(GA-A) (170°C for P(GA-MA)). TGA of free GA-based polymers presented one three-step thermal degradation behavior. All the studied polymers exhibited a final weight percentage loss around 80%. Currently, we have no explanation to explain these results. Supplementary experiments will be planned in the near future to investigate the degradation mechanism of such novel P(GA-A) and P(GA-MA) polymers.

Antioxidant activity of free GA-based polymers

As GA is one of the best natural antioxidants, we expect that polymers carrying free GA moiety in each monomer unit (P(GA-A) and P(GA-MA)) exhibit such property. To demonstrate that, we first carried out DPPH radical scavenging assays with deprotected polymers or with GA as model. The antioxidant activity of GA and of the free-GA based polymers turned down the DPPH absorbance, and was easily observed as the colour of the solution changed instantly from purple (DPPH) to yellow upon DPPH disappearance according to Scheme 3 leading to very stable radical forms of GA.[59] As the concentration of GA or GA-based monomer unit increased, the absorption of DPPH of the mixture at 517 nm (absorption maximum wavelength) dropped gradually to reach a plateau after 12 minutes of reaction. On the contrary, the color of the DPPH solution didn't change when adding perbenzylated polymers (not shown). While protected polymers showed no signs of an antioxidant activity, all free GA-based polymers actively exhibit excellent antioxidant activity.

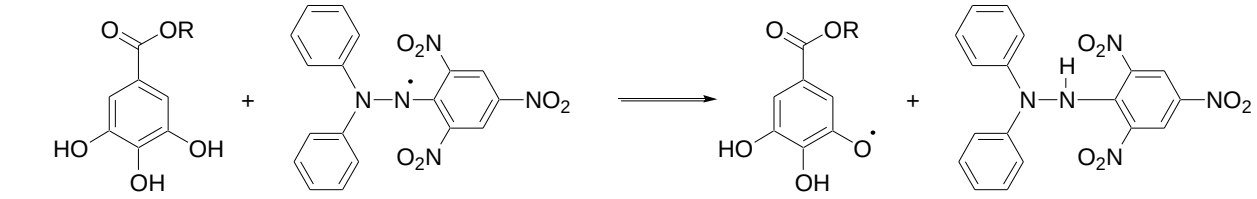

Scheme 3. Reaction between DPPH and GA or GA-based monomer unit.

The absorption decreases with respect to the concentration of the tested antioxidants and the percentage of reduced DPPH are represented in figures 8A and 8B, respectively. P(GA-A) and P(GA-MA) generated likewise DPPH radicals scavenging behaviour whereas lower concentrations of GA were administrated to achieve similar DPPH mixture absorptions (Figure

8A). This is demonstrated by the values of the critical concentration (C_{50}) at which 50% of the initial DPPH radicals are reduced. As shown in Figure 8B, the percentage of scavenged DPPH radicals was proportional to the concentrations of GA or GA repeating units up to high degrees of reduction in a linear mode. With our experimental conditions, C_{50} of GA was registered at about 8 μM. The free GA-based polymers produced in the present study showed higher C_{50} values at about 13.5 μM and 14.5 μM of GA-based monomer units for P(GA-A) and P(GA-MA), respectively. Nevertheless, P(GA-A) and P(GA-MA) demonstrated a marginally better antioxidant activity than the previously reported polyvinylgallol (C_{50} = 32μM of gallol-based monomer units) and similar activity to gallol (C_{50} = 16.3 μM).[44] Such advantage can be accredited to the spacer between each polyphenol group and the chain backbone in P(GA-A) and P(GA-MA) granting a higher mobility of such a group compared to gallol one in the previously reported polyvinylgallol. The lower antioxidant properties of free GA-based polymers *vs* GA was attributed to the lower accessibility of adjacent GA monomer units due to the steric hindrance from the polymeric chains, in agreement with litterature.[44]

Another method to evaluate the antioxidant activity of free GA-based polymers is to study the oxygen uptake inhibition during the oxidation of methyl linoleate initiated by AIBN.[62] Usually, methyl linoleate can undergo oxidation in the presence of radicals and oxygen (Figure S12) but this oxidation may be inhibited in the presence of an antioxidant. Initially, the oxidation of methyl linoleate was studied through the monitoring of the evolution of the pressure of O_2 ($\Delta P = P_0(O_2) - P_{2.5hours}(O_2)$) in the reactor (Figure 8C). The oxygen uptake inhibition index (OUI, Figure 8D) was plotted according to equation 2. Assays were performed in the presence of GA as model, P(GA-A) and P(GA-MA) using the same molar concentration of GA moiety. As shown, GA caused the inhibition percentage of 75% after 2.5 hours, whereas those of P(GA-A) and

P(GA-MA) were similar at 55% at the same time. The difference of values between GA and free GA-based polymers can nevertheless be explained by the low solubility of the polymers in the reaction medium as 1-butanol is the common used solvent to carry out this experiment but does not dissolve P(GA-A) and P(GA-MA). In such a case, DMSO was consequently added in the medium to keep the polymers soluble, whereas GA is highly soluble in both solvents. Nevertheless, such results mirror the ones obtained from the study of the reduction of DPPH radicals and confirm the antioxidant property of (GA-A) and P(GA-MA).

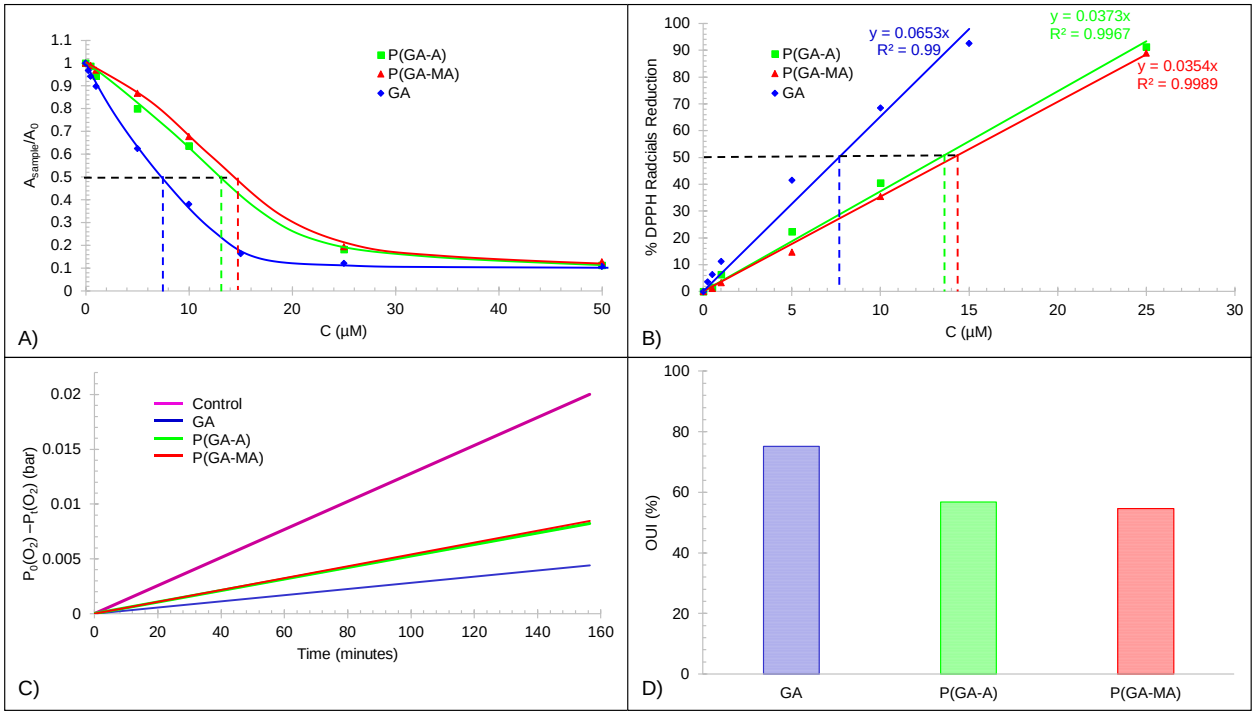

Figure 8. Antioxidant activity of GA and of free GA-based polymers (P(GA-A) and P(GA-MA). Evolutions of A) the relative absorbance values of the DPPH/antioxidant system in MeOH, B) the percentage of reduced DPPH radical *vs* the concentration of the GA or GA-monomer units, C) the pressure difference ($P_0(O_2)$- $P_t(O_2)$) in the reactor containing methyl linoleate, AIBN and antioxidant and D) the antioxidant uptake inhibition index (OUI) of GA/GA-based polymers

CONCLUSION

Novel GA-based acrylate and methacrylate were prepared according to a multistep strategy to further allow their radical polymerization. Photo-mediated RAFT polymerization was herein selected as a low-energy, spatio and temporal controlled technique where its efficiency was investigated depending on the monomer and the choice of CTA. Contrary to the acrylate one, perbenzylated GA-based methacrylate was proved to be polymerized in a controlled manner with an adequate choice of chain transfer agent. Later on, hydrogenolysis of these (meth)acrylic polymers under mild conditions readily resulted in free GA-based polymers.

The antioxidant efficiency of these free GA-based polymers was studied in comparison with that of gallic acid, showing a very efficient scavenging of DPPH radicals. Similarly, the inhibition of methyl linoleate oxidation by free GA-based polymers was proven and compared to that of GA. In accordance with these properties and their thermal characteristics, such free GA-based polymers can be used as bioactive thermoplastic packaging in food industry for instance. Moreover, we believe that these antioxidant bio-based polymers will also be of interest for various applications in cosmetics or in pharmaceutical domain for instance.

ASSOCIATED CONTENT

Supporting Information. ^{1}H NMR and J-mod ^{13}C NMR spectra. ATR-FTIR spectra. Equations used to estimate the conversion. SEC traces. Photo-induced decomposition of TPO-L, then initiation of the polymerization. TGA thermograms. Oxidation of methyl linoleate.

AUTHOR INFORMATION

Corresponding Author

Correspondance to Jean-Luc Six (E-mail: jean-luc.six@univ-lorraine.fr) and Christine Gérardin-Charbonnier (E-mail: christine.gerardin@univ-lorraine.fr).

Author Contributions

The manuscript was written through contributions of all authors. All authors have given approval to the final version of the manuscript.

ACKNOWLEDGMENT

The authors thank i) the ‘‘Impact Biomolecules’’ project of the ‘‘Lorraine Université d’Excellence’’ (Investissements d’avenir –ANR-15-IDEX-04-LUE) fund and ii) the Energy Mechanics Processes Products research department of the Université de Lorraine for the financial support. The authors thank Olivier Fabre (LCPM) for NMR characterization, Alexandre Collar (LCPM) for SEC characterization, Jean-Claude Sivault (LCPM) for homemade UV-VIS LED lamp development, and Béatrice Georges (LERMAB) for the antioxidant tests.

REFERENCES

1. Newman, D. J.; Cragg, G. M., Natural Products as Sources of New Drugs over the Nearly Four Decades from 01/1981 to 09/2019. *Journal of Natural Products* **2020,** *83* (3), 770-803.
2. Lautié, E.; Russo, O.; Ducrot, P.; Boutin, J. A., Unraveling Plant Natural Chemical Diversity for Drug Discovery Purposes. *Frontiers in pharmacology* **2020,** *11*, 397-397.
3. Wright, G. D., Opportunities for natural products in 21st century antibiotic discovery. *Natural Product Reports* **2017,** *34* (7), 694-701.
4. Gonçalves, J.; Ramos, R.; Luís, Â.; Rocha, S.; Rosado, T.; Gallardo, E.; Duarte, A. P., Assessment of the Bioaccessibility and Bioavailability of the Phenolic Compounds of Prunus avium L. by in Vitro Digestion and Cell Model. *ACS Omega* **2019,** *4* (4), 7605-7613.

5. Tsimogiannis, D.; Oreopoulou, V., Chapter 16 - Classification of Phenolic Compounds in Plants. In *Polyphenols in Plants (Second Edition)*, Watson, R. R., Ed. Academic Press: 2019; pp 263-284.
6. Roy, M.; Datta, A., Fundamentals of Phytochemicals. In *Cancer Genetics and Therapeutics: Focus on Phytochemicals*, Springer Singapore: Singapore, 2019; pp 49-81.
7. Panzella, L., Natural Phenolic Compounds for Health, Food and Cosmetic Applications. *Antioxidants* **2020,** *9* (5), Article ID 427.
8. Arroyo, B. J.; Santos, A. P.; de Almeida de Melo, E.; Campos, A.; Lins, L.; Boyano-Orozco, L. C., Chapter 8 - Bioactive Compounds and Their Potential Use as Ingredients for Food and Its Application in Food Packaging. In *Bioactive Compounds*, Campos, M. R. S., Ed. Woodhead Publishing: 2019; pp 143-156.
9. Kumar, N.; Gupta, S.; Chand Yadav, T.; Pruthi, V.; Kumar Varadwaj, P.; Goel, N., Extrapolation of phenolic compounds as multi-target agents against cancer and inflammation. *Journal of Biomolecular Structure and Dynamics* **2019,** *37* (9), 2355-2369.
10. Mark, R.; Lyu, X.; Lee, J. J. L.; Parra-Saldívar, R.; Chen, W. N., Sustainable production of natural phenolics for functional food applications. *Journal of Functional Foods* **2019,** *57*, 233-254.
11. Subramanian, A. P.; John, A. A.; Vellayappan, M. V.; Balaji, A.; Jaganathan, S. K.; Supriyanto, E.; Yusof, M., Gallic acid: prospects and molecular mechanisms of its anticancer activity. *RSC Advances* **2015,** *5* (45), 35608-35621.
12. Dróżdż, P.; Pyrzynska, K., Extracts from pine and oak barks: phenolics, minerals and antioxidant potential. *International Journal of Environmental Analytical Chemistry* **2019**, 1-9.
13. Zhang, B.; Cai, J.; Duan, C.-Q.; Reeves, M. J.; He, F., A Review of Polyphenolics in Oak Woods. *International Journal of Molecular Sciences* **2015,** *16* (4), 6978-7014.
14. Uddin, S. J.; Afroz, M.; Zihad, S. M. N. K.; Rahman, M. S.; Akter, S.; Khan, I. N.; Al-Rabbi, S. M. S.; Rouf, R.; Islam, M. T.; Shilpi, J. A.; Nahar, L.; Tiralongo, E.; Sarker, S. D., A Systematic Review on Anti-diabetic and Cardioprotective Potential of Gallic Acid: A Widespread Dietary Phytoconstituent. *Food Reviews International* **2020**, 1-20.
15. Shabani, S.; Rabiei, Z.; Amini-Khoei, H., Exploring the multifaceted neuroprotective actions of gallic acid: a review. *International Journal of Food Properties* **2020,** *23* (1), 736-752.
16. Kahkeshani, N.; Farzaei, F.; Fotouhi, M.; Alavi, S. S.; Bahramsoltani, R.; Naseri, R.; Momtaz, S.; Abbasabadi, Z.; Rahimi, R.; Farzaei, M. H.; Bishayee, A., Pharmacological effects of gallic acid in health and diseases: A mechanistic review. *Iranian journal of basic medical sciences* **2019,** *22* (3), 225-237.
17. Bhattacharyya, S.; Ahammed, S. M.; Saha, B. P.; Mukherjee, P. K., The Gallic Acid–Phospholipid Complex Improved the Antioxidant Potential of Gallic Acid by Enhancing Its Bioavailability. *AAPS PharmSciTech* **2013,** *14* (3), 1025-1033.
18. Goszcz, K.; Deakin, S. J.; Duthie, G. G.; Stewart, D.; Megson, I. L., Bioavailable Concentrations of Delphinidin and Its Metabolite, Gallic Acid, Induce Antioxidant Protection Associated with Increased Intracellular Glutathione in Cultured Endothelial Cells. *Oxidative Medicine and Cellular Longevity* **2017**, Article ID 9260701.
19. Ferruzzi, M. G.; Lobo, J. K.; Janle, E. M.; Cooper, B.; Simon, J. E.; Wu, Q.-L.; Welch, C.; Ho, L.; Weaver, C.; Pasinetti, G. M., Bioavailability of Gallic Acid and Catechins from Grape Seed Polyphenol Extract is Improved by Repeated Dosing in Rats: Implications for Treatment in Alzheimer's Disease. *Journal of Alzheimer's Disease* **2009,** *18*, 113-124.

20. Chuysinuan, P.; Chimnoi, N.; Techasakul, S.; Supaphol, P., Gallic Acid-Loaded Electrospun Poly(L-Lactic Acid) Fiber Mats and their Release Characteristic. **2009,** *210* (10), 814-822.
21. Ghitescu, R.-E.; Popa, A.-M.; Popa, V. I.; Rossi, R. M.; Fortunato, G., Encapsulation of polyphenols into pHEMA e-spun fibers and determination of their antioxidant activities. *International Journal of Pharmaceutics* **2015,** *494* (1), 278-287.
22. Aydogdu, A.; Sumnu, G.; Sahin, S., Fabrication of gallic acid loaded Hydroxypropyl methylcellulose nanofibers by electrospinning technique as active packaging material. *Carbohydrate polymers* **2019,** *208*, 241-250.
23. Chebil, A.; Léonard, M.; Six, J.-L.; Nouvel, C.; Durand, A., Nanoparticulate delivery systems for alkyl gallates: Influence of the elaboration process on particle characteristics, drug encapsulation and in-vitro release. *Colloids and Surfaces B: Biointerfaces* **2018,** *162*, 351-361.
24. Chebil, A.; Funfschilling, D.; Six, J.-L.; Nouvel, C.; Durand, A.; Léonard, M., Process conditions for preparing well-defined nano- and microparticles as delivery systems of alkyl gallates. *Particuology* **2019,** *44*, 105-116.
25. Thanyacharoen, T.; Chuysinuan, P.; Techasakul, S.; Nooeaid, P.; Ummartyotin, S., Development of a gallic acid-loaded chitosan and polyvinyl alcohol hydrogel composite: Release characteristics and antioxidant activity. *International Journal of Biological Macromolecules* **2018,** *107*, 363-370.
26. Li, J.; Kim, S. Y.; Chen, X.; Park, H. J., Calcium-alginate beads loaded with gallic acid: Preparation and characterization. *LWT - Food Science and Technology* **2016,** *68*, 667-673.
27. Behl, G.; Sharma, M.; Sikka, M.; Dahiya, S.; Chhikara, A.; Chopra, M., Gallic acid loaded disulfide cross-linked biocompatible polymeric nanogels as controlled release system: synthesis, characterization, and antioxidant activity. *Journal of Biomaterials Science, Polymer Edition* **2013,** *24* (7), 865-881.
28. Pinho, E.; Henriques, M.; Soares, G., Cyclodextrin/cellulose hydrogel with gallic acid to prevent wound infection. *Cellulose* **2014,** *21* (6), 4519-4530.
29. Aouf, C.; Nouailhas, H.; Fache, M.; Caillol, S.; Boutevin, B.; Fulcrand, H., Multi-functionalization of gallic acid. Synthesis of a novel bio-based epoxy resin. *European Polymer Journal* **2013,** *49* (6), 1185-1195.
30. Ma, S.; Jiang, Y.; Liu, X.; Fan, L.; Zhu, J., Bio-based tetrafunctional crosslink agent from gallic acid and its enhanced soybean oil-based UV-cured coatings with high performance. *RSC Advances* **2014,** *4* (44), 23036-23042.
31. Shim, J.; Kim, L.; Kim, H. J.; Jeong, D.; Lee, J. H.; Lee, J.-C., All-solid-state lithium metal battery with solid polymer electrolytes based on polysiloxane crosslinked by modified natural gallic acid. *Polymer* **2017,** *122*, 222-231.
32. Tarzia, A.; Montanaro, J.; Casiello, M.; Annese, C.; Nacci, A.; Maffezzoli, A., Synthesis, Curing, and Properties of an Epoxy Resin Derived from Gallic Acid. *BioResources* **2017,** *13* (1), 632-645.
33. Ren, L.; Ma, X.; Zhang, J.; Qiang, T., Preparation of gallic acid modified waterborne polyurethane made from bio-based polyol. *Polymer* **2020,** *194*, Article ID 122370.
34. Can, M.; Bulut, E.; Özacar, M., Synthesis and Characterization of Gallic Acid Resin and Its Interaction with Palladium(II), Rhodium(III) Chloro Complexes. *Industrial & Engineering Chemistry Research* **2012,** *51* (17), 6052-6063.

35. Uemura, Y.; Shimasaki, T.; Teramoto, N.; Shibata, M., Thermal and mechanical properties of bio-based polymer networks by thiol-ene photopolymerizations of gallic acid and pyrogallol derivatives. *Journal of Polymer Research* **2016,** *23* (10), Article ID 216.
36. Li, X.; Su, Y.; Chen, Q.; Lin, Y.; Tong, Y.; Li, Y., Synthesis and Characterization of Biodegradable Hyperbranched Poly(ester-amide)s Based on Natural Material. *Biomacromolecules* **2005,** *6* (6), 3181-3188.
37. Reina, A.; Gerken, A.; Zemann, U.; Kricheldorf, H. R., New polymer syntheses, 101. Liquid-crystalline hyperbranched and potentially biodegradable polyesters based on phloretic acid and gallic acid. *Macromol. Chem. Phys.* **1999,** *200* (7), 1784-1791.
38. Kricheldorf, H. R.; Stukenbrock, T., New polymer syntheses XCIII. Hyperbranched homo- and copolyesters derived from gallic acid and β-(4-hydroxyphenyl)-propionic acid. *Journal of Polymer Science: Part A: Polymer Chemistry* **1998,** *36* (13), 2347-2357.
39. Liu, J.; Yong, H.; Liu, Y.; Bai, R., Recent advances in the preparation, structural characteristics, biological properties and applications of gallic acid grafted polysaccharides. *International Journal of Biological Macromolecules* **2020,** *156*, 1539-1555.
40. Yan, M.; Li, B.; Zhao, X.; Yi, J., Physicochemical properties of gelatin gels from walleye pollock (Theragra chalcogramma) skin cross-linked by gallic acid and rutin. *Food Hydrocolloids* **2011,** *25* (5), 907-914.
41. Spizzirri, U. G.; Iemma, F.; Puoci, F.; Cirillo, G.; Curcio, M.; Parisi, O. I.; Picci, N., Synthesis of Antioxidant Polymers by Grafting of Gallic Acid and Catechin on Gelatin. *Biomacromolecules* **2009,** *10* (7), 1923-1930.
42. Romero-Montero, A.; del Valle, L. J.; Puiggalí, J.; Montiel, C.; García-Arrazola, R.; Gimeno, M., Poly(gallic acid)-coated polycaprolactone inhibits oxidative stress in epithelial cells. *Materials Science and Engineering: C* **2020,** *115*, Article ID 111154.
43. Hlushko, R.; Hlushko, H.; Sukhishvili, S. A., A family of linear phenolic polymers with controlled hydrophobicity, adsorption and antioxidant properties. *Polymer Chemistry* **2018,** *9* (4), 506-516.
44. Zhan, K.; Ejima, H.; Yoshie, N., Antioxidant and Adsorption Properties of Bioinspired Phenolic Polymers: A Comparative Study of Catechol and Gallol. *ACS Sustainable Chemistry & Engineering* **2016,** *4* (7), 3857-3863.
45. Zhan, K.; Kim, C.; Sung, K.; Ejima, H.; Yoshie, N., Tunicate-Inspired Gallol Polymers for Underwater Adhesive: A Comparative Study of Catechol and Gallol. *Biomacromolecules* **2017,** *18* (9), 2959-2966.
46. Patil, N.; Cordella, D.; Aqil, A.; Debuigne, A.; Admassie, S.; Jérôme, C.; Detrembleur, C., Surface- and Redox-Active Multifunctional Polyphenol-Derived Poly(ionic liquid)s: Controlled Synthesis and Characterization. *Macromolecules* **2016,** *49* (20), 7676-7691.
47. Pan, X.; Tasdelen, M. A.; Laun, J.; Junkers, T.; Yagci, Y.; Matyjaszewski, K., Photomediated controlled radical polymerization. *Progress in Polymer Science* **2016,** *62*, 73-125.
48. Moad, G.; Rizzardo, E., A 20th anniversary perspective on the life of RAFT (RAFT coming of age). *Polymer International* **2020,** *69*, 658-661.
49. Perrier, S., 50th Anniversary Perspective: RAFT Polymerization—A User Guide. *Macromolecules* **2017,** *50* (19), 7433-7447.
50. Ferji, K.; Venturini, P.; Cleymand, F.; Chassenieux, C.; Six, J.-L., In situ glyco-nanostructure formulation via photo-polymerization induced self-assembly. *Polymer Chemistry* **2018,** *9* (21), 2868-2872.

51. Ikkene, D.; Arteni, A. A.; Song, H.; Laroui, H.; Six, J. L.; Ferji, K., Synthesis of dextran-based chain transfer agent for RAFT-mediated polymerization and glyco-nanoobjects formulation. *Carbohydrate Polymers* **2020,** *234*, Article ID 115943.
52. Ikkene, D.; Arteni, A. A.; Ouldali, M.; Six, J.-L.; Ferji, K., Self-assembly of amphiphilic copolymers containing polysaccharide: PISA versus nanoprecipitation, and the temperature effect. *Polymer Chemistry* **2020,** *11* (29), 4729-4740.
53. Lu, L.; Zhang, H.; Yang, N.; Cai, Y., Toward Rapid and Well-Controlled Ambient Temperature RAFT Polymerization under UV−Vis Radiation: Effect of Radiation Wave Range. *Macromolecules* **2006,** *39* (11), 3770-3776.
54. McKenzie, T. G.; Fu, Q.; Uchiyama, M.; Satoh, K.; Xu, J.; Boyer, C.; Kamigaito, M.; Qiao, G. G., Beyond Traditional RAFT: Alternative Activation of Thiocarbonylthio Compounds for Controlled Polymerization. *Adv. Sci.* **2016,** *3* (9), Article ID 1500394.
55. Liu, F.; Long, Y.; Zhao, Q.; Liu, X.; Qiu, G.; Zhang, L.; Ling, Q.; Gu, H., Gallol-containing homopolymers and block copolymers: ROMP synthesis and gelation properties by metal-coordination and oxidation. *Polymer* **2018,** *143*, 212-227.
56. Lertturongchai, P.; Ibrahim, M. I. A.; Durand, A.; Sunintaboon, P.; Ferji, K., Synthesis of Thermoresponsive Copolymers with Tunable UCST-Type Phase Transition Using Aqueous Photo-RAFT Polymerization. *Macromolecular Rapid Communications* **2020,** *41* (9), Article ID 2000058.
57. Li, H.; Li, M.; Xu, R.; Wang, S.; Zhang, Y.; Zhang, L.; Zhou, D.; Xiao, S., Synthesis, structure activity relationship and in vitro anti-influenza virus activity of novel polyphenol-pentacyclic triterpene conjugates. *European Journal of Medicinal Chemistry* **2019,** *163*, 560-568.
58. Ren, Y.; Himmeldirk, K.; Chen, X., Synthesis and Structure−Activity Relationship Study of Antidiabetic Penta-O-galloyl-d-glucopyranose and Its Analogues. *Journal of Medicinal Chemistry* **2006,** *49* (9), 2829-2837.
59. Rigoussen, A.; Verge, P.; Raquez, J.-M.; Dubois, P., Natural Phenolic Antioxidants As a Source of Biocompatibilizers for Immiscible Polymer Blends. *ACS Sustainable Chemistry & Engineering* **2018,** *6* (10), 13349-13357.
60. Nomeir, B.; Fabre, O.; Ferji, K., Effect of Tertiary Amines on the Photoinduced Electron Transfer-Reversible Addition–Fragmentation Chain Transfer (PET-RAFT) Polymerization. *Macromolecules* **2019,** *52* (18), 6898-6903.
61. Ikkene, D.; Arteni, A. A.; Ouldali, M.; Francius, G.; Brûlet, A.; Six, J.-L.; Ferji, K., Direct Access to Polysaccharide-Based Vesicles with a Tunable Membrane Thickness in a Large Concentration Window via Polymerization-Induced Self-Assembly. *Biomacromolecules* **2021,** *22* (7), 3128-3137.
62. Poaty, B.; Dumarçay, S.; Gérardin, P.; Perrin, D., Modification of grape seed and wood tannins to lipophilic antioxidant derivatives. *Industrial Crops and Products* **2010,** *31* (3), 509-515.